Ionospheric Correction for retrieving atmospheric variables from GPS occultation data

Cheng-Yung Huang[1] and Yuei-An Liou[1, 2]

1. National Space Organization, 8F, 9 Prosperity 1st Road, Hsinchu Science Park, Hsinchu 30078, Taiwan, yusn@nspo.org.tw
2. Center for Space and Remote Sensing Research, National Central University, Chung-Li 320, Taiwan. Email: yueian@csrsr.ncu.edu.tw

Abstract

[1] There are systematical errors associated with ionospheric influence in retrieving key atmospheric parameters from radio occultation (RO) soundings. In order to obtain better-quality retrievals, we develop a new method, hereafter called National Central University Radio Occultation (NCURO) scheme, to reduce the ionospheric influence. The excess phase is divided into two parts, namely geometric excess length and path excess length (excess length along ray path due to refractivity effect). An excess phase equation is presented and implemented in the NCURO scheme whose performance is evaluated through comparisons with model simulation and experimental data. The model simulation is based on the use of the ionospheric model IRI2001 and atmospheric model NRLMSISE-00. Results show that the NCURO scheme significantly reduces the ionospheric influence at altitudes above 70 km as does the scheme presented in the literature, and provides better corrections for the atmospheric profile. INDEX TERMS: 2400 Ionosphere: Ionosphere; 6964 Radio Science: Radio wave propagation; 6969 Radio Science: Remote sensing.

1. Introduction

[2] Since 1995, the GPS radio occultation (RO) technique has been used for retrieving Earth's profiles of refractivity, temperature, pressure and water vapor in the neutral atmosphere and electron density in the ionosphere [*Liou et al.*, 2005]. A variety of retrieval schemes and correction methods are hence developed to perform the retrieval.

[3] However, systematic errors exist and degrade the retrieval accuracy of atmospheric parameters when the RO technique is implemented. The errors are caused by many factors, such as large-scale horizontal gradients [*Ahmad and Tyler*, 1999], small-scale irregularity, super refraction [*Sokolovskiy*, 2003], gravity wave [*Liou et al.* 2002, 2003, 2004; *Pavelyev et al.*, 2003], multipath [*Igarashi et al.*, 2000; *Ao et al.*, 2003], reflected signals from surface [*Pavelyev et al.*, 2002], oblateness of earth [*Syndergaard*, 1998], and ionospheric influence [*Syndergaard*, 2000, 2002].

[4] To reduce the ionospheric influence, ionosphere-free linear combination is generally used to derive the neutral atmospheric parameters. Four ionospheric correction methods were discussed by Gorbunov [2002]: 1) the linear combination of the excess phase at the same sample time, 2) the linear combination of the phase modulations at the common ray perigee height, 3) the linear combination of the phase of the Doppler shifts at the same sample time, 4) the linear combination of the refraction angles at the common impact parameter. The linear combination of refraction angle takes the following form [Vorob'ev and Krasil'nikova, 1994]

$$\varepsilon_{1,2}(p) = \frac{f_1^2 \varepsilon_1(p) - f_2^2 \varepsilon_2(p)}{f_1^2 - f_2^2}, \quad (1)$$

where ε is the bending angle and p is the impact parameter, f is the carrier frequency of GPS signals, and subscripts 1 and 2 represent L1 and L2 signals, respectively. In this study, the two rules of linear combinations of phase paths (ε) at the same time (p=t) and the linear combinations of phase paths at the same impact parameter (p=a) were compared with Syndergaard's and our new ionospheric correction methods. The same processes for bending angles were also carried out. Here, the excess phases corrected as function of time and impact parameter are represented by Lc(t) and Lc(a), respectively.

[5] In this paper, we consider only the systematic errors connected with the ionospheric influence. A new method (thereafter called NCURO scheme) is developed for the ionosphere correction. Its performance is compared with that of the method proposed by *Syndergaard* [2000, 2002]. The NCURO method consists in presentation of excess phases at two GPS frequencies as a sum of geometric delay and path delay. The equations describing the L1 or L2 signal delays are modified. Ray-tracing is used to quantify the geometric delay and path delay in simulations.

2. NCURO Algorithm Derivation

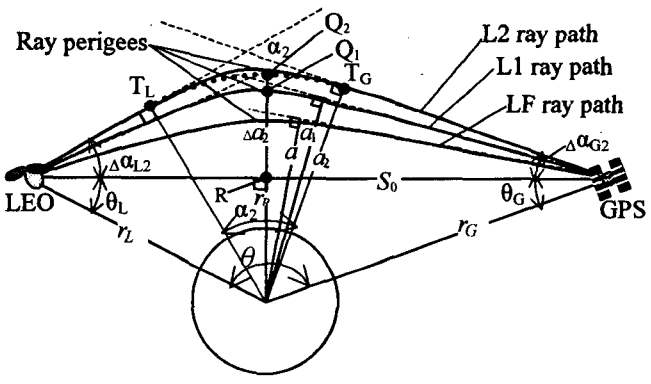

Figure 1. Illustration of ray path separation and pictorial definition of some parameters. Dash lines LEO-Q_1-GPS and LEO-Q_2-GPS can be approximated by geometric delays of L1 and L2 signals for ionospheric delay calibration.

[6] We derive a method to correct the phase path of the bending effect caused by electron density gradient. The phase path between GPS and LEO can be described by [*Pavelyev et al.*, 2004]

$$L = \sqrt{r_G^2 - a^2} + \sqrt{r_L^2 - a^2} + a\alpha(a) + \int_a^\infty \alpha(a')da', \quad (2)$$

where r_G and r_L are the distances from earth center to GPS and LEO, respectively, and α is the bending angle between the two ray directions transmitted from GPS and received by LEO. The sum of the first three terms is considered as the geometric delay, and the fourth term as the path delay. The first term is the length from GPS to point T_L, the second term is the length from LEO to point T_G, and the third term is the arc length of circle. The radius of the circle is equal to impact parameter. The radian of arc is equal to the bending angle. The geometric delay defined by equation (2) is suitable to describe the geometric length of the ray path when the bending angle is not very big and the refractivity at the perigee point of the ray path is weak.

[7] If the refractive index ($n = 1+10^{-6}N$) approximates to 1, $\ln(n) \sim N$ and $nr \sim r$, the path delay of the fourth term in equation (2) can be rewritten as

$$\begin{aligned}\int_a^\infty \alpha(a')da' &= \int_a^\infty \frac{2dn}{nd(nr)}\sqrt{(nr)^2-a^2}\,d(nr) \\ &\cong \int_a^\infty \frac{2N(r)r}{\sqrt{r^2-a^2}}dr = \int_a^\infty N(r)ds_0(r)\end{aligned} \tag{3}$$

where n is equal to 1 at GPS and LEO positions. The s_0 is the length between GPS and LEO in vacuum. The path delay is proportional to f^{-2} when the bending angle caused by ionosphere is proportional to f^{-2}.

[8] The geometric length minus straight line (S_0) between GPS and LEO can be described as

$$\begin{aligned}&G-S_0 \\ &=(R_G\cos(\theta_G+\Delta\alpha_G)+R_L\cos(\theta_L+\Delta\alpha_L)) \\ &+R_G\sin(\theta_G+\Delta\alpha_G)\Delta\alpha_G+R_L\sin(\theta_L+\Delta\alpha_L)\Delta\alpha_L-(D_{GR}+D_{LR}) \\ &=[0.5D_{GR}(\Delta\alpha_G)^2-(1/3)r_0(\Delta\alpha_G)^3+\cdots] \\ &+[0.5D_{LR}(\Delta\alpha_L)^2-(1/3)r_0(\Delta\alpha_L)^3+\cdots]\end{aligned}, \tag{4}$$

where D_{LR} is the distance from LEO to point R, D_{GR} is the distance from GPS to point R in Figure 1, $_\Delta\alpha_L$ is the bending angle between the signal vector received by LEO and the vector from GPS to LEO, $_\Delta\alpha_L$ is the bending angle between signal vector transmitted from GPS and the vector from GPS to LEO, and r_o is the distance from Earth center to the tangent point(R) of the ray path in vacuum. If the higher order (>2) terms are ignored, the geometric delay approximates to the sum of lengths of two lines, from GPS to point Q and from point Q to LEO, when the cube of bending angle is much smaller than the square of bending angle. The differential impact parameter $_\Delta a$ will be approximately equal to $D_{LR}\times_\Delta\alpha_L$ or $D_{LG}\times_\Delta\alpha_G$ and also equal to $(a-r_0)$.

[9] The bending angles are contributed by two factors associated with refractivity gradients in the neutral atmosphere (NEU) and ionosphere (ION). If the bending angle due to higher order terms is ignored, equation (4) becomes

$$G-S_0 = 0.5D_R\left(\alpha_{NEU}^2+2\alpha_{NEU}\alpha_{ION}+\alpha_{ION}^2\right), \tag{5}$$

where $1/D_R = 1/D_{GR}+1/D_{LR}$. The bending angle caused by the electron density gradient is proportional to f^{-2} [*Vorob'ev and Krasil'nikova*, 1994]. Hence, the third term (α^2_{ION}) of equation (5) due to ionospheric effect is proportional to f^{-4}, and the second term ($2\alpha_{NEU}\times\alpha_{ION}$) is proportional to f^{-2}. The third term becomes dominant geometric delay as bending angle (α_{NEU}) is relatively small compared with bending angle (α_{ION}). Therefore, the geometric delay is proportional to f^{-4}.

Corrected ionospheric delay

[10] The formula for ionospheric delay correction suggested by *Syndergaard* [2000] is

$$\tilde{L}_c(a) = s_0 \mp \frac{K\langle B_\parallel\rangle_0}{f_1f_2(f_1+f_2)}\gamma_0+\frac{1}{2}\frac{C}{f_1^2f_2^2}\Gamma, \tag{6}$$

where $\gamma_0 = \int N_e ds_0$ is the total electron content (TEC) along the LF ray path, $\langle B_\parallel\rangle_0 = \gamma_0^{-1}\int N_e B_\parallel ds_0$ is the weighted mean value of the geomagnetic field along the LF ray path, $s_0 = \int n ds_0$ is the integrated length along the LF ray path, Γ is a function of N_e along the path, and the LF means the ionospheric free ray path. The detail about this ionospheric correction method is referred to [*Syndergaard, 2000, 2002*]

[11] According to equations (3) and (5), the delay caused by ionosphere can be separated into two parts: path delay and geometric delay. The two kinds of ionosphere delays may be corrected separately. The path delay is proportional to f^{-2} so that it can be corrected by

$$\begin{aligned}Lc_{NCURD}(a) = &\left\{\frac{f_1^2(L_1(a)-G_1(a))-f_2^2(L_2(a)-G_2(a))}{f_1^2-f_2^2}\right\}. \\ &+\left\{\frac{1}{2}\left(\frac{1}{D_G}+\frac{1}{D_L}\right)(a_1-a_{ION})^2\right\}\end{aligned} \tag{7}$$

where $_\Delta a_{ION} = (_\Delta a_1 - _\Delta a_2)/(1-f_1^2/f_2^2)$, $_\Delta a_1 = a_1 - r_o$. The path delay and geometric delay of equations (7) are calculated as function of the impact parameter.

4. Results

4.1 Simulation performance

[12] To assess the effectiveness of ionospheric corrections on various delay components, we begin with model simulations. Background refractivity is obtained using the ionospheric model IRI2001 and atmospheric model NRLMISI-00 by ray tracing method. The ionospheric refractive index is given by [Bassiri and Hajj, 1993]:

$$n = 1-\frac{1}{2}X\pm\frac{1}{2}XY|\cos\theta|-\frac{1}{8}X^2-\frac{1}{4}XY^2(1+\cos^2\theta)-\cdots, \tag{8}$$

where θ is the angle between the magnetic field and ray direction, $X = N_e e^2/m\varepsilon_0\omega^2$, $Y = eB/m\omega$, ω is the carrier angular frequency, e is elementary charge, m is the mass of electron, ε_0 is the free space permittivity, and N_e is the electron density. The four refractivity indices were integrated along ray path separately; $DN=10^{-6}\int Nds$ is the neutral atmosphere delay along the ray path, $DX=-1/2\int Xds$ is the electron density delay along ray path, $DYL=\pm1/2\int XY|\cos\theta|ds$ is the magnetic delay contributed from the magnetic field parallel to the ray path, and DG is the geometric delay caused by the bending effect of ray path.

[13] Figure 2 shows (a) phase residuals and (b) bending angle caused by the four components of interest by using the

ionosphere-free combination, and (c) percentage of the bending angle perpendicular versus parallel to the occultation plane. The 3-D ray tracing technique is implemented. The occultation plane is defined by GPS and LEO positions and radial vector of the occultation point. The bending angle between transmitted signal vector parallel to occultation plane and received signal vector parallel to occultation plane is defined as parallel bending angle, whose orthogonal component is defined as perpendicular bending angle. The perpendicular bending angle is due to refractivity gradient perpendicular to the occultation plane.

[14] It is observed that the phase residual and bending angle can be corrected better with the same impact parameter than the same received time by comparing the DX(a) and DX(t) curves in Figure 2. This is because the perigee points of L1 and L2 ray paths are much closer for the former case. In addition, the main error source due to geometric delay comes from ionosphere at altitudes near 100 Km. From the DYL curve, the bending angle due to magnetic field can be ignored compared to the other elements. Furthermore, it is seen that the contribution from the perpendicular part cannot be ignored at altitude above 100 km.

[15] Note that there is an obvious difference in phase residual and bending angle between the two calibration methods only for the DX component. Hence, we plot results of phase residuals and bending angles with same impact height only for the DX case, but not for the other cases.

[16] Of the four delay components, DX and portion of DG (due to neutral atmospheric effect) contain information of ray bending. That is, the other terms are simply to cause errors to the retrievals when the RO technique is implemented. Since their magnitudes are large enough to significantly degrade the retrievals at altitudes above 40 km, correction to their impact parameters must be implemented. Results from various correction methods are presented below.

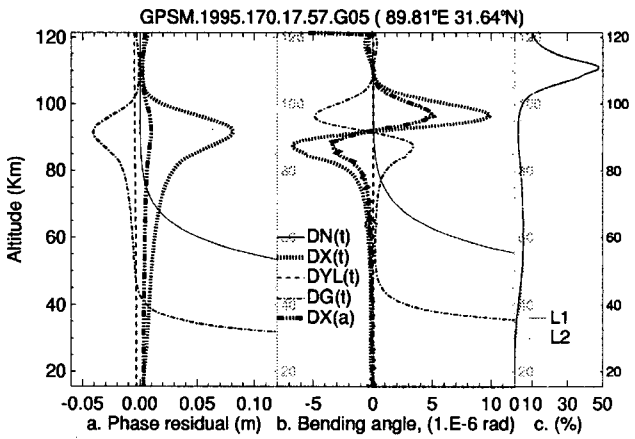

Figure 2. (a) Phase residuals and (b) bending angle from the ionosphere-free combination, and (c) percentage of the bending angle perpendicular versus parallel to the occultation plane.

4.2 Real Data Performance

[17] Results of implementing four ionospheric delay correction methods are shown in Figure 3. The four methods are: traditional ionosphere-free combination corrected with same sample time (Lc(t)) and with same impact height (Lc(a)); the use of equation (6) proposed by *Syndergaard* [2000] (Lc(Γ)); and the use of equation (7) proposed by the NCURO scheme (Lc(NCU)). Results from each method are plotted by two curves – solid and dash curves. The solid curves are retrieved from the observation data while the dash curves are recovered from simulations (by the ray-tracing method). The dash curves are shifted downward by 0.02 m for easy comparison and lower paired curves are shifted downward by 0.1 m in sequence for comparison. The impact parameters must be calculated before the ionospheric-free combinations were processed for Lc(a), the fourth term (Γ) of equation (6) and the NCURO scheme. The impact parameters of two frequencies were calculated separately at their own sample time. Because the ionospheric corrected excess phase is calculated at equal impact parameter, the L2 excess is interpolated to the L1 impact parameter. When the impact parameters were calculated, the smooth scheme is used, while no smooth scheme is performed during ionospheric-free combination processes.

[18] It is observed that Lc(t) and Lc(a) solid curves exhibit a clear ridge and a trough, respectively, around 93 km. The ridge and trough may be due to E layer's refractivity gradient. They are not seen for the other two curves, and indicate that both the Syndergaard method and the NCURO scheme perform well to correct ionosphere influence. The fluctuations of the curves around 115 Km are due to the ambiguity cycle slip. It is still a challenging task to resolve these fluctuations, and not further discussed in this paper.

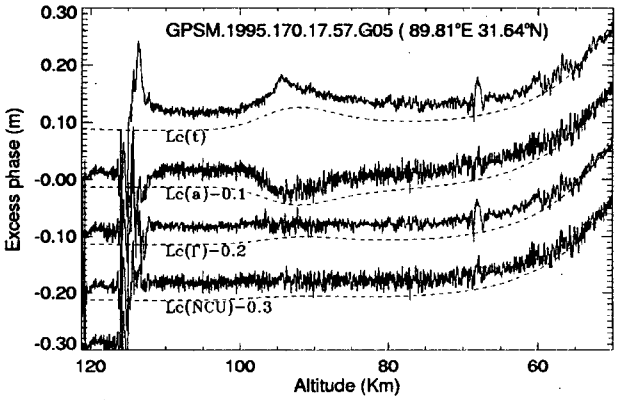

Figure 3. Excess phase from four ionospheric calibration methods. Solid curves are retrieved from occultation observation data, and dash curves from simulation. Lower paired curves are shifted downward by 0.1 m in sequence for comparison.

[19] Figure 4 shows results from the other one occultation event. There is one region with strong fluctuations around 100~80 Km for the top two curves. The strong fluctuations are caused by ionospheric activities when the rays propagate through the ionosphere. They will degrade the accuracy of retrievals and, hence, must be removed. It is clearly seen that these fluctuations are removed when the NCURO scheme is used as seen on the fourth curve. When the Syndergaard method is applied as seen on the third curve, the larger scale fluctuations are almost removed, but not the small scale fluctuations. The random noise of Lc(a) and NCURO scheme is slightly increased as compared to the Lc(t) and Lc(Γ), it might be due to the interpolation process of impact parameters of two frequencies. The distance of ray path perigees of L1 and L2 are closer at the same impact parameter than that at same sample time. From the comparisons of equations (6) and (7) and the results of Figure 4 and Figure 5, we suggest the space coherent fluctuation can be removed by the NCURO scheme, while the

time coherent fluctuation can be removed by the Syndergaard method.

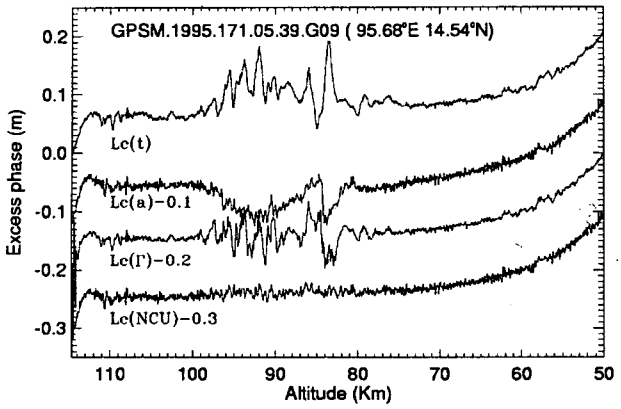

Figure 4. Excess phases from four ionospheric correction methods. The lower curves are shifted downward by 0.1 m in sequence for comparison.

5. Conclusions

[21] Simulation is performed to study the ionospheric correction using the traditional ionosphere-free combination for retrieving atmospheric parameters. We show that the correction with the same impact parameter performs better than that with the same sample time. Nevertheless, the geometric delay caused by ionosphere at some altitudes associated with ionospheric activities cannot be corrected appropriately by the Lc(a) and Lc(t) ionosphere-free combination.

In addition, it is shown that ray path delay and geometric delay can be corrected separately. The equations to characterize the delays are derived and implemented in the presented NCURO approach. The performance of the NCURO scheme appears to be superior to the ionospheric correction methods in the literature by use of theoretical ray tracing simulations and experimental data comparisons. Specifically, two experimental data sets are utilized. It shall be of great interest to further verify the developed scheme by using more experimental sets. In near future, the developed scheme will be implemented for the FORMOSAT3/COSMIC mission

[19] **Acknowledgments.** We are grateful to UCAR for the access of the GPS/MET data, and National Space Organization of Taiwan for financial support under the grant 92-NSPO(B)-RS3-FA07-03.

References

Ao, C.O., G.A. Hajj , T. Meehan, S.S.Leroy, E.R. Kursinski, M. de la Torre Juarez, B.A. Iijima,and A.J. Mannucci, 2003, Backpropagation Processing of GPS Radio Occultation Data, First CHAMP Mission Results for Gravity, Magnetic and Atmospheric Studies, Springer, Series, ISBN 3-540-00206-5, 415-422.

Ahmad, B. and G. L. Tyler, 1999, Systematic errors in atmospheric profiles obtained from Abelian inversion of radio occultation data: Effect of large-scale horizontal gradients, JGR, Vol. 104, No. D4, 3971-3992.

Bassiri, S. G. A. Hajj, 1993, Higher-order ionospheric effects on the global positioning system observables and means of modeling them, manuscripta geodaetica, 18, 280-289.

Gorbunov, M. E., 2002, Ionospheric correction and statistical optimization of radio occultation data, Radio Science, Vol. 37, NO. 5, 1084, 17-1~17-9.

Igarashi A. Pavelyev, K. Hocke, D. Pavelyev, I. A. Kucherjavenkov, S. Matyugov, A. Zakharov, O. Yakovlev., 2000, Radio holographic principle for observing natural processes in the atmosphere and retrieving meteorological parameters from radio occultation data. Earth Planets Space, No. 52, 893-899.

Liou, Y.-A., A.G. Pavelyev, C.-Y. Huang, K. Igarashi, and K. Hocke, 2002, Simultaneous observation of the vertical gradients of refractivity in the atmosphere and electron density in the lower ionosphere by radio occultation amplitude method. Geophysical Research Letters, Vol. 29, No. 19, 43-1-43-4, doi:10.1029/2002GL015155.

Liou, Y.-A., A.G. Pavelyev, C.-Y. Huang, K. Igarashi, K. Hocke, and S.-K. Yan, 2003, An analytic method for observing the gravity waves using radio occultation data. Geophysical Research Letters, Vol. 30, no. 20, 2021. doi: 10.1029/2003GL017818.

Liou, Y.-A., A.G. Pavelyev, J. Wickert, C.-Y. Huang, S.-K. Yan, S.-F. Liou, 2004, Response of GPS occultation signals to atmospheric gravity waves and retrieval of gravity wave parameters. GPS Solutions, 8, 103-111. (DOI: 10.1007/s10291-004-0090-x)

Liou, Y.A., A.G. Pavelyev, J. Wickert, T. Schmidt, and A.A. Pavelyev, 2005, Analysis of Atmospheric and Ionospheric Structures using the GPS/MET and CHAMP Radio Occultation Database: a Methodological Review. GPS Solutions, 9(2).

NSSDC, Space physics model, http://nssdc.gsfc.nasa.gov/space/model/

Pavelyev A.G., Y.-A. Liou, C. Reigber, J. Wickert, K. Igarashi, K. Hocke, C.Y. Huang, 2002: GPS radio holography as a tool for remote sensing of the atmosphere and mesosphere from space. GPS Solutions, 100-108, Vol. 6, No. 1-2.

Pavelyev A.G., T. Tsuda, K. Igarashi, Y.-A. Liou, and K. Hocke, 2003, Wave structures in the electron density profile in the ionospheric D and E-layers observed by radio holography analysis of the GPS/MET radio occultation data. J. Atmos. Solar-Terr. Phys., 65(1), 59-70.

Pavelyev, A. G., Y. A. Liou, J. Wickert, 2004, Diffractive vector and scalar integrals for bistatic radio holographic remote sensing, Radio Science, Vol. 39, RS4011.

Sokolovskiy, S., 2003, Effect of superrefraction on inversions of radio occultation signals in the lower troposphere, Radio Sci., 38(3), 1058, doi:10.1029/2002RS002728.

Syndergaard, S., 1998, Modeling the Impact of the Earths Oblateness on the Retrieval of Temperature and Pressure Profiles from Limb Sounding, J. Atmos. Solar-Terr. Phys., 60, 171-180.

Syndergaard, S., 2000, On the Ionosphere Calibration in GPS Radio Occultation Measurements, Radio Sci., 35, 865-883.

Syndergaard, S., 2002, A New Algorithm for Retrieving GPS Radio Occultation Total Electron Content, Geophys. Res. Lett. 29, 16, 2001GL014478.

Vorob'ev, V. V., and T. G. Krasil'nikova, 1994, Estimation of the accuracy of the atmospheric refractive index recovery from Doppler shift measurements at frequencies used in the NAVSTAR system, Phys. Atmos. Ocean, 29, 602-609.